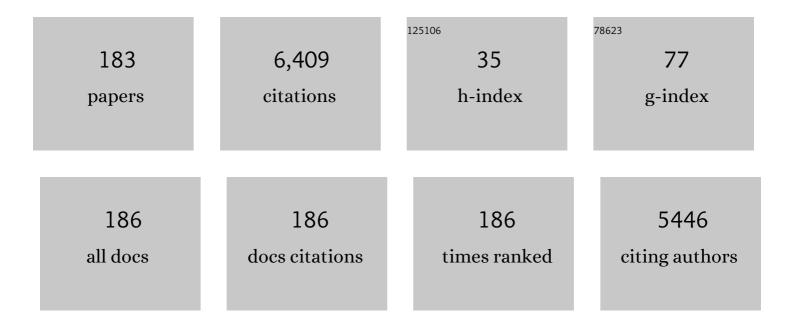
List of Publications by Year in descending order

Source: https://exaly.com/author-pdf/3699614/publications.pdf Version: 2024-02-01



RDAM HOFY

#	Article	IF	CITATIONS
1	Technoâ€economic analysis of the use of atomic layer deposited transition metal oxides in silicon heterojunction solar cells. Progress in Photovoltaics: Research and Applications, 2023, 31, 414-428.	4.4	11
2	Tubeâ€ŧype plasmaâ€enhanced atomic layer deposition of aluminum oxide: Enabling record lab performance for the industry with demonstrated cell efficiencies >24%. Progress in Photovoltaics: Research and Applications, 2023, 31, 52-61.	4.4	1
3	9.6%-Efficient all-inorganic Sb ₂ (S,Se) ₃ solar cells with a MnS hole-transporting layer. Journal of Materials Chemistry A, 2022, 10, 2835-2841.	5.2	19
4	Large volume tomography using plasma FIB-SEM: A comprehensive case study on black silicon. Ultramicroscopy, 2022, 233, 113458.	0.8	4
5	Quantifying the Effect of Nanofeature Size on the Electrical Performance of Black Silicon Emitter by Nanoscale Modeling. IEEE Journal of Photovoltaics, 2022, 12, 744-753.	1.5	4
6	Converting Sewage Water into H2 Fuel Gas Using Cu/CuO Nanoporous Photocatalytic Electrodes. Materials, 2022, 15, 1489.	1.3	26
7	Increased Efficiency of Organic Solar Cells by Seeded Control of the Molecular Morphology in the Active Layer. Solar Rrl, 2022, 6, .	3.1	5
8	Recent Advances in Materials Design Using Atomic Layer Deposition for Energy Applications. Advanced Functional Materials, 2022, 32, .	7.8	34
9	Designing 3d metal oxides: selecting optimal density functionals for strongly correlated materials. Physical Chemistry Chemical Physics, 2022, 24, 14119-14139.	1.3	4
10	Zinc oxide family semiconductors for ultraviolet radiation emission – A cathodoluminescence study. Materials Research Bulletin, 2022, 153, 111906.	2.7	2
11	Impact of Substrate Thickness on the Degradation in Multicrystalline Silicon. IEEE Journal of Photovoltaics, 2021, 11, 65-72.	1.5	10
12	Understanding Light- and Elevated Temperature-Induced Degradation in Silicon Wafers Using Hydrogen Effusion Mass Spectroscopy. IEEE Journal of Photovoltaics, 2021, 11, 1363-1369.	1.5	9
13	Progress in Semitransparent Organic Solar Cells. Solar Rrl, 2021, 5, 2100041.	3.1	44
14	On the Enhanced Phosphorus Doping of Nanotextured Black Silicon. IEEE Journal of Photovoltaics, 2021, 11, 298-305.	1.5	13
15	Impact of Pregrown SiO _{<i>x</i>} on the Carrier Selectivity and Thermal Stability of Molybdenum-Oxide-Passivated Contact for Si Solar Cells. ACS Applied Materials & Interfaces, 2021, 13, 36426-36435.	4.0	8
16	Field-Effect Passivation of Undiffused Black Silicon Surfaces. IEEE Journal of Photovoltaics, 2021, 11, 897-907.	1.5	4
17	Doped Nickel Oxide Carrier-Selective Contact for Silicon Solar Cells. IEEE Journal of Photovoltaics, 2021, 11, 1176-1187.	1.5	10
18	Silicon Nanotexture Surface Area Mapping Using Ultraviolet Reflectance. IEEE Journal of Photovoltaics, 2021, 11, 1291-1298.	1.5	3

BRAM HOEX

#	Article	IF	CITATIONS
19	A novel passivating electron contact for high-performance silicon solar cells by ALD Al-doped TiO2. Solar Energy, 2021, 228, 531-539.	2.9	23
20	Atomic layer deposition enabling higher efficiency solar cells: A review. Nano Materials Science, 2020, 2, 204-226.	3.9	44
21	Controlling Light- and Elevated-Temperature-Induced Degradation With Thin Film Barrier Layers. IEEE Journal of Photovoltaics, 2020, 10, 19-27.	1.5	23
22	Investigation of light-induced degradation in N-Type silicon heterojunction solar cells during illuminated annealing at elevated temperatures. Solar Energy Materials and Solar Cells, 2020, 218, 110752.	3.0	19
23	Interface Modification Enabled by Atomic Layer Deposited Ultraâ€Thin Titanium Oxide for Highâ€Efficiency and Semitransparent Organic Solar Cells. Solar Rrl, 2020, 4, 2000497.	3.1	15
24	Bilayer MoO _{<i>X</i>} /CrO _X Passivating Contact Targeting Highly Stable Silicon Heterojunction Solar Cells. ACS Applied Materials & Interfaces, 2020, 12, 36778-36786.	4.0	28
25	Highâ€Efficiency Nonfullerene Organic Solar Cells Enabled by Atomic Layer Deposited Zirconiumâ€Doped Zinc Oxide. Solar Rrl, 2020, 4, 2000241.	3.1	18
26	3D characterisation using plasma FIB-SEM: A large-area tomography technique for complex surfaces like black silicon. Ultramicroscopy, 2020, 218, 113084.	0.8	12
27	Optimized Ni _{1â^'x} Al _x O hole transport layer for silicon solar cells. RSC Advances, 2020, 10, 22377-22386.	1.7	1
28	Understanding Field-Effect Passivation of Black Silicon: Modeling Charge Carrier Population Control in Compressed Space Charge Regions. , 2020, , .		1
29	Impact of wafer properties and production processes on the degradation in industrial PERC solar cells. , 2020, , .		1
30	Graded NixAlyO hole transport layer in silicon solar cells. , 2020, , .		0
31	(Invited) ALD Enabling High-Efficiency Solar Cells. ECS Meeting Abstracts, 2020, MA2020-02, 1669-1669.	0.0	0
32	Cd-Free Cu ₂ ZnSnS ₄ solar cell with an efficiency greater than 10% enabled by Al ₂ O ₃ passivation layers. Energy and Environmental Science, 2019, 12, 2751-2764.	15.6	112
33	Large-area MACE Si nano-inverted-pyramids for PERC solar cell application. Solar Energy, 2019, 188, 300-304.	2.9	37
34	15% Efficiency Ultrathin Silicon Solar Cells with Fluorine-Doped Titanium Oxide and Chemically Tailored Poly(3,4-ethylenedioxythiophene):Poly(styrenesulfonate) as Asymmetric Heterocontact. ACS Nano, 2019, 13, 6356-6362.	7.3	53
35	Evaluating the Impact of SiN _x Thickness on Lifetime Degradation in Silicon. IEEE Journal of Photovoltaics, 2019, 9, 601-607.	1.5	36
36	Atomic Layer Deposited AlxNiyO as Hole Selective Contact for Silicon Solar Cells. , 2019, , .		1

 $\label{eq:action} \ensuremath{\mathsf{Atomic}}\xspace \ensuremath{\mathsf{Layer}}\xspace \ensuremath{\mathsf{Deposited}}\xspace \ensuremath{\mathsf{AlxNiyO}}\xspace \ensuremath{\mathsf{Selective}}\xspace \ensuremath{\mathsf{Contact}}\xspace \ensuremath{\mathsf{for}}\xspace \ensuremath{\mathsf{Solar}}\xspace \ensuremath{\mathsf{Contact}}\xspace \ensuremath{\mathsf{for}}\xspace \ensuremath{\mathsf{Solar}}\xspace \ensuremath{\mathsf{Contact}}\xspace \ensuremath{\mathsf{for}}\xspace \ensuremath{\mathsf{Solar}}\xspace \ensuremath{\mathsf{Contact}}\xspace \ensuremath{\mathsf{for}}\xspace \ensuremath{\mathsf{Solar}}\xspace \ensuremath{\mathsf{Contact}}\xspace \ensuremath{\mathsf{for}}\xspace \ensuremath{\mathsf{Contact}}\xspace \ensuremath{\mathsf{for}}\xspace \ensuremath{\mathsf{Solar}}\xspace \ensuremath{\mathsf{Contact}}\xspace \ensuremath{\mathsf{for}}\xspace \ensuremath{\mathsf{Solar}}\xspace \ensuremath{\mathsf{Contact}}\xspace \ensuremath{\mathsf{for}}\xspace \ensuremath{\mathsf{Solar}}\xspace \ensuremath{\mathsf{Contact}}\xspace \ensuremath{\mathsf{for}}\xspace \ensuremath$ 36

#	Article	IF	CITATIONS
37	High-efficient Cd-free CZTS solar cells achieved by nanoscale atomic layer deposited aluminium oxide. , 2019, , .		0
38	Advanced Characterisation of Black Silicon Surface Topography with 3D PFIB-SEM. , 2019, , .		2
39	Efficient light harvesting in hybrid quantum dot–interdigitated back contact solar cells <i>via</i> resonant energy transfer and luminescent downshifting. Nanoscale, 2019, 11, 18837-18844.	2.8	15
40	<i>In situ</i> x-ray photoelectron emission analysis of the thermal stability of atomic layer deposited WOx as hole-selective contacts for Si solar cells. Journal of Vacuum Science and Technology A: Vacuum, Surfaces and Films, 2018, 36, .	0.9	8
41	Minimising bulk lifetime degradation during the processing of interdigitated back contact silicon solar cells. Progress in Photovoltaics: Research and Applications, 2018, 26, 38-47.	4.4	25
42	Influence of dielectric passivation layer thickness on LeTID in multicrystalline silicon. , 2018, , .		5
43	Tunnel Oxides Formed by Field-induced Anodization for Silicon Solar Cell Passivation. , 2018, , .		0
44	Contact properties of electroless nickel plated contacts on diffused p+ silicon surfaces , 2018, , .		0
45	Atomic layer deposited ZnxNi1â^'xO: A thermally stable hole selective contact for silicon solar cells. Applied Physics Letters, 2018, 113, .	1.5	17
46	ALD ZnSnO buffer layer for enhancing heterojunction interface quality of CZTS solar cells. , 2018, , .		0
47	Evaluating the Impact of Thermal Annealing on Al <inf>2</inf> O <inf>3</inf> /c-Si Interface Properties by Non-Destructive Measurements. , 2018, , .		0
48	Quantifying optical losses of silicon solar cells with carrier selective hole contacts. AlP Conference Proceedings, 2018, , .	0.3	1
49	Enhanced Heterojunction Interface Quality To Achieve 9.3% Efficient Cd-Free Cu ₂ ZnSnS ₄ Solar Cells Using Atomic Layer Deposition ZnSnO Buffer Layer. Chemistry of Materials, 2018, 30, 7860-7871.	3.2	66
50	Thermal stability analysis of WOx and MoOx as hole-selective contacts for Si solar cells using in situ XPS. AIP Conference Proceedings, 2018, , .	0.3	7
51	Evaluating the impact of thermal annealing on <i>c</i> -Si/Al2O3 interface: Correlating electronic properties to infrared absorption. AlP Advances, 2018, 8, .	0.6	10
52	Improving the Silicon Surface Passivation by Aluminum Oxide Grown Using a Nonâ€₽yrophoric Aluminum Precursor. Physica Status Solidi - Rapid Research Letters, 2018, 12, 1800156.	1.2	3
53	Investigation of the thermal stability of MoOx as hole-selective contacts for Si solar cells. Journal of Applied Physics, 2018, 124, 073106.	1.1	35
54	Mie resonators as rearside light trapping structures in planar crystalline silicon solar cells. , 2018, , .		1

#	Article	IF	CITATIONS
55	Material properties of AlOx for silicon surface passivation. , 2018, , 27-40.		0
56	The role of hydrogenation and gettering in enhancing the efficiency of nextâ€generation Si solar cells: An industrial perspective. Physica Status Solidi (A) Applications and Materials Science, 2017, 214, 1700305.	0.8	59
57	Dielectric surface passivation for silicon solar cells: A review. Physica Status Solidi (A) Applications and Materials Science, 2017, 214, 1700293.	0.8	188
58	Numerical Simulation of Doping Process by BBr3 Tube Diffusion for Industrial n -Type Silicon Wafer Solar Cells. IEEE Journal of Photovoltaics, 2017, 7, 755-762.	1.5	13
59	The effects of bifacial deposition of ALD AlOx on the contact properties of screen-printed contacts for p-type PERC solar cells. Energy Procedia, 2017, 124, 914-921.	1.8	6
60	Characterisation of thermal annealed WO <i> _x </i> on p-type silicon for hole-selective contacts. Japanese Journal of Applied Physics, 2017, 56, 08MA08.	0.8	12
61	Extracting dielectric fixed charge density on highly doped crystalline-silicon surfaces using photoconductance measurements. Journal of Applied Physics, 2017, 122, 195301.	1.1	0
62	The Effect of Bifacial AlOx Deposition on PERC Solar Cell Performance. IEEE Journal of Photovoltaics, 2017, 7, 1528-1535.	1.5	8
63	POCl3 diffusion for industrial Si solar cell emitter formation. Frontiers in Energy, 2017, 11, 42-51.	1.2	38
64	Improved understanding of the recombination rate at inverted p ⁺ silicon surfaces. Japanese Journal of Applied Physics, 2017, 56, 08MB05.	0.8	3
65	Extracting the fixed charge density in HfOx films grown on highly-doped p-Si samples. , 2017, , .		0
66	Unintentional consequences of dual mode plasma reactors: Implications for upscaling lab-record silicon surface passivation by silicon nitride. Japanese Journal of Applied Physics, 2017, 56, 08MB12.	0.8	2
67	Acceleration and mitigation of carrier-induced degradation in p-type multi-crystalline silicon. Physica Status Solidi - Rapid Research Letters, 2016, 10, 237-241.	1.2	71
68	Empirical and Quokka simulated evidence for enhanced V <inf>OC</inf> due to limited junction area for high efficiency silicon solar cells. , 2016, , .		1
69	Rapid passivation of carrier-induced defects in p-type multi-crystalline silicon. Solar Energy Materials and Solar Cells, 2016, 158, 102-106.	3.0	49
70	Ultrathin Silicon Solar Cell Loss Analysis. IEEE Journal of Photovoltaics, 2016, 6, 1160-1166.	1.5	2
71	Investigation of laser ablation on boron emitters for <i>n</i> â€ŧype rearâ€junction PERT type silicon wafer solar cells. Progress in Photovoltaics: Research and Applications, 2015, 23, 1706-1714.	4.4	8
72	0.4% absolute efficiency increase for inline-diffused screen-printed multicrystalline silicon wafer solar cells by non-acidic deep emitter etch-back. Solar Energy Materials and Solar Cells, 2015, 137, 193-201.	3.0	11

#	Article	IF	CITATIONS
73	Quantification of Front Side Metallization Area on Silicon Wafer Solar Cells for Background Plating Detection. Energy Procedia, 2015, 77, 717-724.	1.8	4
74	Progress with surface passivation of heavily doped n+ silicon by industrial PECVD SiNx films. , 2015, , .		4
75	Resistive Intrinsic ZnO Films Deposited by Ultrafast Spatial ALD for PV Applications. IEEE Journal of Photovoltaics, 2015, 5, 1462-1469.	1.5	15
76	Extraction of Surface Recombination Velocity at Highly Doped Silicon Surfaces Using Electron-Beam-Induced Current. IEEE Journal of Photovoltaics, 2015, 5, 263-268.	1.5	9
77	Passivation of Boron-Doped Industrial Silicon Emitters by Thermal Atomic Layer Deposited Titanium Oxide. IEEE Journal of Photovoltaics, 2015, 5, 1062-1066.	1.5	41
78	Dielectric Charge Tailoring in PECVD SiO <inline-formula> <tex-math>\${}_x\$</tex-math> </inline-formula> /SiN <inline-formula> <tex-math>\${}_x\$</tex-math> </inline-formula> Stacks and Application at the Rear of Al Local Back Surface Field Si Wafer Solar Cells. IEEE Journal of Photovoltaics, 2015, 5, 1014-1019.	1.5	13
79	A Systematic Loss Analysis Method for Rear-Passivated Silicon Solar Cells. IEEE Journal of Photovoltaics, 2015, 5, 619-626.	1.5	53
80	Accurate extraction of the series resistance of aluminum local back surface field silicon wafer solar cells. Solar Energy Materials and Solar Cells, 2015, 133, 113-118.	3.0	6
81	Excellent <i>c</i> -Si surface passivation by low-temperature atomic layer deposited titanium oxide. Applied Physics Letters, 2014, 104, .	1.5	126
82	SunsPZ©: Real-time spatially resolved solar cell parameter visualizer. , 2014, , .		0
83	Accurate potential drop sheet resistance measurements of laser-doped areas in semiconductors. Journal of Applied Physics, 2014, 116, 134505.	1.1	2
84	Numerical analysis of injection level dependent effective lifetime on 125 mm undiffused lifetime samples. , 2014, , .		3
85	Excellent surface passivation of heavily doped p+ silicon by low-temperature plasma-deposited SiOx/SiNy dielectric stacks with optimised antireflective performance for solar cell application. Solar Energy Materials and Solar Cells, 2014, 120, 204-208.	3.0	26
86	Extremely low surface recombination velocities on lowâ€resistivity <i>n</i> â€type and <i>p</i> â€type crystalline silicon using dynamically deposited remote plasma silicon nitride films. Progress in Photovoltaics: Research and Applications, 2014, 22, 641-647.	4.4	32
87	A novel approach to investigate bulk carrier lifetime using low frequency fluctuation noise measurement. Semiconductor Science and Technology, 2014, 29, 125005.	1.0	1
88	Electrical and Microstructural Analysis of Contact Formation on Lightly Doped Phosphorus Emitters Using Thick-Film Ag Screen Printing Pastes. IEEE Journal of Photovoltaics, 2014, 4, 168-174.	1.5	31
89	Black silicon: fabrication methods, properties and solar energy applications. Energy and Environmental Science, 2014, 7, 3223-3263.	15.6	396
90	Laser Chemical Processing of n-Type Emitters for Solid-Phase Crystallized Polysilicon Thin-Film Solar Cells. IEEE Journal of Photovoltaics, 2014, 4, 1445-1451.	1.5	0

#	Article	IF	CITATIONS
91	Optical Modeling of Alkaline Saw-Damage-Etched Rear Surfaces of Monocrystalline Silicon Solar Cells. IEEE Journal of Photovoltaics, 2014, 4, 1436-1444.	1.5	5
92	Impact of Auger recombination parameterisations on predicting silicon wafer solar cell performance. Journal of Computational Electronics, 2014, 13, 647-656.	1.3	8
93	Geometric confinement of directly deposited features on hydrophilic rough surfaces using a sacrificial layer. Journal of Materials Science, 2014, 49, 4363-4370.	1.7	3
94	Two-dimensional numerical simulation of boron diffusion for pyramidally textured silicon. Journal of Applied Physics, 2014, 116, 184103.	1.1	6
95	Excellent boron emitter passivation for highâ€efficiency Si wafer solar cells using AlO <i>_x</i> /SiN <i>_x</i> dielectric stacks deposited in an industrial inline plasma reactor. Progress in Photovoltaics: Research and Applications, 2013, 21, 760-764.	4.4	24
96	Numerical Modelling of Silicon p+ Emitters Passivated by a PECVD AlOx/SiNx Stack. Energy Procedia, 2013, 33, 104-109.	1.8	8
97	Investigation of Screen-Printed Rear Contacts for Aluminum Local Back Surface Field Silicon Wafer Solar Cells. IEEE Journal of Photovoltaics, 2013, 3, 690-696.	1.5	11
98	A Fill Factor Loss Analysis Method for Silicon Wafer Solar Cells. IEEE Journal of Photovoltaics, 2013, 3, 1170-1177.	1.5	119
99	Progress in Surface Passivation of Heavily Doped n-Type and p-Type Silicon by Plasma-Deposited AlO \$_{m x}\$/SiN\$_{m x}\$ Dielectric Stacks. IEEE Journal of Photovoltaics, 2013, 3, 1163-1169.	1.5	21
100	Direct Laser Doping of Poly-Silicon Thin Films Via Laser Chemical Processing. IEEE Journal of Photovoltaics, 2013, 3, 1259-1264.	1.5	1
101	Accurate characterization of thin films on rough surfaces by spectroscopic ellipsometry. Thin Solid Films, 2013, 545, 451-457.	0.8	11
102	Advanced Solar Cell Modelling. Energy Procedia, 2013, 33, 99-103.	1.8	1
103	Deposition temperature independent excellent passivation of highly boron doped silicon emitters by thermal atomic layer deposited Al2O3. Journal of Applied Physics, 2013, 114, 094505.	1.1	18
104	Numerical Analysis of p Emitters Passivated by a PECVD AlOx/SiNx Stack. Energy Procedia, 2013, 38, 124-130.	1.8	6
105	On the transient amorphous silicon structures during solid phase crystallization. Journal of Non-Crystalline Solids, 2013, 363, 172-177.	1.5	1
106	Laser Chemical Processing (LCP) of Poly-Silicon Thin Film on Glass Substrates. Energy Procedia, 2013, 33, 137-142.	1.8	3
107	Integration of β-FeSi2 with poly-Si on glass for thin-film photovoltaic applications. RSC Advances, 2013, 3, 7733.	1.7	16
108	Medium range order engineering in amorphous silicon thin films for solid phase crystallization. Journal of Applied Physics, 2013, 113, 193511.	1.1	3

#	Article	IF	CITATIONS
109	Broken metal fingers in silicon wafer solar cells and PV modules. Solar Energy Materials and Solar Cells, 2013, 108, 78-81.	3.0	70
110	Extremely low surface recombination velocities on heavily doped planar and textured p ⁺ silicon using low-temperature positively-charged PECVD SiOx/SiNx dielectric stacks with optimised antireflective properties. , 2013, , .		3
111	Excellent <i>c</i> -Si surface passivation by thermal atomic layer deposited aluminum oxide after industrial firing activation. Journal Physics D: Applied Physics, 2013, 46, 385102.	1.3	19
112	Unexpectedly High Etching Rate of Highly Doped n-Type Crystalline Silicon in Hydrofluoric Acid. ECS Journal of Solid State Science and Technology, 2013, 2, P380-P383.	0.9	9
113	The effect of light soaking on crystalline silicon surface passivation by atomic layer deposited Al2O3. Journal of Applied Physics, 2013, 113, .	1.1	55
114	C-Si surface passivation by aluminum oxide studied with electron energy loss spectroscopy. , 2013, , .		1
115	Excellent surface passivation of silicon at low cost: Atomic layer deposited aluminium oxide from solar grade TMA. , 2013, , .		3
116	Identification of geometrically necessary dislocations in solid phase crystallized poly-Si. Journal of Applied Physics, 2013, 114, 043511.	1.1	7
117	Extracting physical properties of arbitrarily shaped laser-doped micro-scale areas in semiconductors. Applied Physics Letters, 2013, 103, .	1.5	3
118	Low-Temperature Surface Passivation of Moderately Doped Crystalline Silicon by Atomic-Layer-Deposited Hafnium Oxide Films. ECS Journal of Solid State Science and Technology, 2013, 2, N11-N14.	0.9	24
119	Silicon surface passivation by aluminium oxide studied with electron energy loss spectroscopy. Physica Status Solidi - Rapid Research Letters, 2013, 7, 937-941.	1.2	29
120	Excellent Passivation of p\$^{+}\$ Silicon Surfaces by Inline Plasma Enhanced Chemical Vapor Deposited SiO\$_{x}\$/AIO\$_{x}\$ Stacks. Japanese Journal of Applied Physics, 2012, 51, 10NA17.	0.8	0
121	Advanced Modelling of Silicon Wafer Solar Cells. Japanese Journal of Applied Physics, 2012, 51, 10NA06.	0.8	1
122	Enhancement of laser-induced rear surface spallation by pyramid textured structures on silicon wafer solar cells. Optics Express, 2012, 20, A984.	1.7	13
123	Advanced modeling of the effective minority carrier lifetime of passivated crystalline silicon wafers. Journal of Applied Physics, 2012, 112, .	1.1	36
124	Aluminum local back surface field solar cells with inkjet-opened rear dielectric films. , 2012, , .		1
125	Investigation of defect luminescence from multicrystalline Si wafer solar cells using Xâ€ray fluorescence and luminescence imaging. Physica Status Solidi - Rapid Research Letters, 2012, 6, 460-462.	1.2	2
126	State-of-the-art surface passivation of boron emitters using inline PECVD AlO <inf>x</inf> /SiN <inf>x</inf> stacks for industrial high-efficiency silicon wafer solar cells. , 2012, ,		4

•

BRAM HOEX

#	Article	IF	CITATIONS
12	Optimised Antireflection Coatings using Silicon Nitride on Textured Silicon Surfaces based on Measurements and Multidimensional Modelling. Energy Procedia, 2012, 15, 78-83.	1.8	128
12	Low-temperature Surface Passivation of Moderately Doped Crystalline Silicon by Atomic-layer-deposited Hafnium Oxide Films. Energy Procedia, 2012, 15, 84-90.	1.8	34
12	Advanced Characterisation of Silicon Wafer Solar Cells. Energy Procedia, 2012, 15, 147-154.	1.8	4
13	Modelling and Simulation of Field-effect Surface Passivation of Crystalline Silicon-based Solar Cells. Energy Procedia, 2012, 15, 155-161.	1.8	4
13	Line-Imaging Spectroscopy for Characterisation of Silicon Wafer Solar Cells. Energy Procedia, 2012, 15, 171-178.	1.8	5
13	Investigation of Evaporated Rear Contacts for Al-LBSF Silicon Wafer Solar Cells. Energy Procedia, 2012, 25, 10-18.	1.8	3
13	Rear-Side Contact Opening by Laser Ablation for Industrial Screen-Printed Aluminium Local Back Surface Field Silicon Wafer Solar Cells. Energy Procedia, 2012, 25, 19-27.	1.8	22
13	Analysing Solar Cells by Circuit Modelling. Energy Procedia, 2012, 25, 28-33.	1.8	14
13	19% Efficient Inline-diffused Large-area Screen-printed Al-LBSF Silicon Wafer Solar Cells. Energy Procedia, 2012, 27, 444-448.	1.8	10
13	Surface passivation of phosphorusâ€diffused n ⁺ â€type emitters by plasmaâ€assisted atomicâ€la deposited Al ₂ O ₃ . Physica Status Solidi - Rapid Research Letters, 2012, 6, 4-6.	ayer 1.2	73
13	Polarisation analysis of luminescence for the characterisation of defects in silicon wafer solar cells. Progress in Photovoltaics: Research and Applications, 2012, 20, 661-669.	4.4	8
13	Kinetic study of solid phase crystallisation of expanding thermal plasma deposited a-Si:H. Thin Solid Films, 2012, 520, 5820-5825.	0.8	5
13	Excellent Passivation of p+Silicon Surfaces by Inline Plasma Enhanced Chemical Vapor Deposited SiOx/AlOxStacks. Japanese Journal of Applied Physics, 2012, 51, 10NA17.	0.8	2
14	Enhancement of laser-induced rear surface spallation by pyramid textured structures on silicon wafer solar cells. Optics Express, 2012, 20, A984-90.	1.7	1
14	Polarization analysis of luminescence for the characterization of silicon wafer solar cells. Applied Physics Letters, 2011, 98, .	1.5	20
14	Accurate characterisation of silicon nitride films on rough silicon surfaces by ellipsometry. Energy Procedia, 2011, 8, 122-127.	1.8	7
14	Advanced loss analysis method for silicon wafer solar cells. Energy Procedia, 2011, 8, 244-249.	1.8	47
14	In-situ X-ray diffraction analysis of the crystallisation of a-SI:H films deposited by the expanding		0

thermal plasma technique., 2011,,.

#	Article	IF	CITATIONS
145	High-quality surface passivation of low-resistivity p-type C-Si by hydrogenated amorphous silicon nitride deposited by industrial-scale microwave PECVD. , 2011, , .		2
146	The \${f ALU}^{+}\$ Concept: \$N\$-Type Silicon Solar Cells With Surface-Passivated Screen-Printed Aluminum-Alloyed Rear Emitter. IEEE Transactions on Electron Devices, 2010, 57, 1966-1971.	1.6	17
147	Influences of oxygen contamination on evaporated poly-Si thin-film solar cells by solid-phase epitaxy. Thin Solid Films, 2010, 518, 4351-4355.	0.8	4
148	Observations on the spectral characteristics of defect luminescence of silicon wafer solar cells. , 2010, , .		9
149	The ALU ⁺ concept: N-type silicon solar cells with surface-passivated screen-printed aluminum-alloyed rear emitter. , 2009, , .		6
150	Stability of Al2O3 and Al2O3/a-SiNx:H stacks for surface passivation of crystalline silicon. Journal of Applied Physics, 2009, 106, .	1.1	145
151	Electric field induced surface passivation of Si by atomic layer deposited Al <inf>2</inf> O <inf>3</inf> studied by optical second-harmonic generation. , 2009, , .		О
152	Crystal quality improvement of solid-phase crystallized evaporated silicon films by in-situ densification anneal. Solar Energy Materials and Solar Cells, 2009, 93, 1116-1119.	3.0	6
153	Silicon surface passivation by hot-wire CVD Si thin films studied by in situ surface spectroscopy. Thin Solid Films, 2009, 517, 3456-3460.	0.8	18
154	Firing stability of atomic layer deposited Al <inf>2</inf> O <inf>3</inf> for c-Si surface passivation. , 2009, , .		8
155	Surface passivation of highâ€efficiency silicon solar cells by atomicâ€layerâ€deposited Al ₂ O ₃ . Progress in Photovoltaics: Research and Applications, 2008, 16, 461-466.	4.4	414
156	Silicon surface passivation by atomic layer deposited Al2O3. Journal of Applied Physics, 2008, 104, .	1.1	415
157	Negative charge and charging dynamics in Al2O3 films on Si characterized by second-harmonic generation. Journal of Applied Physics, 2008, 104, .	1.1	131
158	On the c-Si surface passivation mechanism by the negative-charge-dielectric Al2O3. Journal of Applied Physics, 2008, 104, .	1.1	479
159	High efficiency n-type Si solar cells on Al2O3-passivated boron emitters. Applied Physics Letters, 2008, 92, .	1.5	316
160	Surface passivation of boron diffused emitters for high efficiency solar cells. , 2008, , .		11
161	Crystalline silicon surface passivation by the negative-charge-dielectric Al <inf>2</inf> 0 <inf>3</inf> . Conference Record of the IEEE Photovoltaic Specialists Conference, 2008, , .	0.0	6
162	Atomic-layer-deposited aluminum oxide for the surface passivation of high-efficiency silicon solar cells. Conference Record of the IEEE Photovoltaic Specialists Conference, 2008, , .	0.0	15

#	Article	IF	CITATIONS
163	Atomic layer deposition: Prospects for solar cell manufacturing. Conference Record of the IEEE Photovoltaic Specialists Conference, 2008 Real-time study of <mml:math <br="" xmlns:mml="http://www.w3.org/1998/Math/MathML">display="inline"><mml:mirow><mml:mi>a</mml:mi><mml:mtext>â^*</mml:mtext><mml:mtext><mml:mi< td=""><td>0.0</td><td>2</td></mml:mi<></mml:mtext></mml:mirow></mml:math>	0.0	2
164	mathvariant="normal">Si <mml:mo>:</mml:mo> <mml:mi mathvariant="normal">H<mml:mo>a^•</mml:mo><mml:mi>c</mml:mi><mml:mtext>a^*</mml:mtext> mathvariant="normal">Siheterointerface formation and epitaxial Si growth by spectroscopic ellipsometry, infrared spectroscopy, and second-harmonic generation.</mml:mi 	knand:mi	40
165	Influence of the Structural and Compositional Properties of PECVD Silicon Nitride as a Passivation Layer for AlGaN HEMTs. ECS Transactions, 2008, 16, 181-191.	0.3	29
166	Excellent passivation of highly doped p-type Si surfaces by the negative-charge-dielectric Al2O3. Applied Physics Letters, 2007, 91, .	1.5	370
167	Optical properties of Y2O3 thin films doped with spatially controlled Er3+ by atomic layer deposition. Journal of Applied Physics, 2007, 101, .	1.1	23
168	Ultralow surface recombination of c-Si substrates passivated by plasma-assisted atomic layer deposited Al2O3. Applied Physics Letters, 2006, 89, 042112.	1.5	646
169	High-Quality Surface Passivation Obtained by High-Rate Deposited Silicon Nitride, Silicon Dioxide and Amorphous Silicon using the Versatile Expanding Thermal Plasma Technique. , 2006, , .		0
170	Good Surface Passivation of C-SI by High Rate Plasma Deposited Silicon Oxide. , 2006, , .		3
171	A Real-Time Study of the a-Si:H/c-Si Interface Formation using Ellipsometry, Infrared Spectroscopy, and Second Harmonic Generation. , 2006, , .		1
172	High-rate plasma-deposited SiO2 films for surface passivation of crystalline silicon. Journal of Vacuum Science and Technology A: Vacuum, Surfaces and Films, 2006, 24, 1823-1830.	0.9	45
173	Interaction of SiH3 radicals with deuterated (hydrogenated) amorphous silicon surfaces. Surface Science, 2005, 598, 35-44.	0.8	20
174	Industrial high-rate (â^1⁄45 nm/s) deposited silicon nitride yielding high-quality bulk and surface passivation under optimum anti-reflection coating conditions. Progress in Photovoltaics: Research and Applications, 2005, 13, 705-712.	4.4	40
175	Hydrogen in Si–Si bond center and platelet-like defect configurations in amorphous hydrogenated silicon. Journal of Vacuum Science & Technology an Official Journal of the American Vacuum Society B, Microelectronics Processing and Phenomena, 2004, 22, 2719.	1.6	20
176	Direct and highly sensitive measurement of defect-related absorption in amorphous silicon thin films by cavity ringdown spectroscopy. Applied Physics Letters, 2004, 84, 3079-3081.	1.5	37
177	Absolute densities of N and excited N2 in a N2 plasma. Applied Physics Letters, 2003, 83, 4918-4920.	1.5	70
178	Thin Film Cavity Ringdown Spectroscopy and Second Harmonic Generation on Thin a-Si:H Films. Materials Research Society Symposia Proceedings, 2003, 762, 1981.	0.1	2
179	Sign reversal of spin polarization inCo/Ru/Al2O3/Comagnetic tunnel junctions. Physical Review B, 2001, 64, .	1.1	50
180	Plasma properties of a novel commercial plasma source for high-throughput processing of c-Si solar cells. , 0, , .		1

#	Article	IF	CITATIONS
181	Controlling the silicon nitride film density for ultrahigh-rate deposition of top quality antireflection coatings. , 0, , .		1
182	Studies into the Growth Mechanism of a-Si:H Usingin situ Cavity Ring-Down Techniques. , 0, , 237-271.		1
183	Plasma Focused Ion Beam Tomography for Accurate Characterization of Black Silicon Validated by Full Wave Optical Simulation. Advanced Materials Technologies, 0, , 2200068.	3.0	0